



Published in final edited form as:

J Immunol. 2015 November 1; 195(9): 4096–4105. doi:10.4049/jimmunol.1500799.

Continuous antigenic stimulation of DO11.10 TCR transgenic mice in the presence or absence of IL-1 β : possible implications for mechanisms of T cell depletion in HIV disease¹

Kristin Ladell^{2,3,*}, Mette D. Hazenberg[†], Mark Fitch[‡], Claire Emson^{‡,§}, Bridget K. McEvoy-Hein Asgarian[‡], Jeff E. Mold^{*}, Corey Miller^{*}, Robert Busch[¶], David A. Price^{||, #}, Marc K. Hellerstein^{‡,§}, and Joseph M. McCune^{3,*}

^{*}Division of Experimental Medicine, University of California, San Francisco, CA, USA

[†]Department of Immunology, University Medical Center Utrecht, Utrecht, The Netherlands

[‡]Department of Nutritional Sciences, University of California, Berkeley, CA USA [§]KineMed Inc.,

Emeryville, CA, USA [¶]Department of Life Sciences, Whitelands College, University of

Roehampton, Parkstead House, London, UK ^{||} Institute of Infection & Immunity, Cardiff University

School of Medicine, Heath Park, Cardiff, UK [#]Vaccine Research Center, National Institute of

Allergy and Infectious Diseases, National Institutes of Health, Bethesda, MD, USA

Abstract

Untreated HIV disease is associated with chronic immune activation and CD4⁺ T cell depletion. A variety of mechanisms have been invoked to account for CD4⁺ T cell depletion in this context, but the quantitative contributions of these proposed mechanisms over time remains unclear. We turned to the DO11.10 TCR transgenic (tg) mouse model, where OVA is recognized in the context of H-2^d, to explore the impact of chronic antigenic stimulation on CD4⁺ T cell dynamics. To model dichotomous states of persistent antigen exposure in the presence or absence of proinflammatory stimulation, we administered OVA peptide (OVAp) to these mice on a continuous basis with or without the prototypic proinflammatory cytokine, interleukin 1 β (IL-1 β). In both cases, circulating antigen-specific and non-specific CD4⁺ T cells were depleted. However, in the absence of IL-1 β , there was limited proliferation and effector/memory conversion of antigen-specific T cells, depletion of peripheral CD4⁺ T cells in hematolymphoid organs, and systemic induction of regulatory FoxP3⁺CD4⁺ T cells, as often observed in late-stage HIV disease. By contrast, when OVAp was administered in the presence of IL-1 β , effector/memory phenotype T cells expanded

¹This work was supported in part by National Institutes of Health Grant RO1 AI43866 (to M.K.H.), European Molecular Biology Organization Grant ALTF 254–2002 (to M.D.H.), and National Institutes of Health Awards U01 AI43641 and R37 AI40312 (to J.M.M.), who is a recipient of the Burroughs Wellcome Fund Clinical Scientist Award in Translational Research and the National Institutes of Health Director's Pioneer Award, part of the National Institutes of Health Roadmap for Medical Research, through Grant DPI OD00329. Funding for the optimization of low-count techniques by mass spectrometry was provided by KineMed Inc. (Emeryville, CA, USA). D.A.P. is a Wellcome Trust Senior Investigator. The Clinical and Translational Science Institute Clinical Research Center was supported by Grant UL1 RR024131-01 from the National Center for Research Resources, a component of the National Institutes of Health, and the National Institutes of Health Roadmap for Medical Research.

³Address correspondence and reprint requests to Joseph M. McCune, M.D., Ph.D., Division of Experimental Medicine, Department of Medicine, University of California, San Francisco, 1001 Potrero Ave., Bldg. 3, Rm. 601, San Francisco, CA, 94110, USA; Phone +1 415-206-8101; mike.mccune@ucsf.edu or Kristin Ladell, M.D., Ph.D., Institute of Infection & Immunity, Cardiff University School of Medicine, Heath Park, Cardiff, CF14 4XN, UK; Phone +44 2920 687 788; ladellk@gmail.com.

²Current address: Institute of Infection & Immunity, Cardiff University School of Medicine, Heath Park, Cardiff, UK.

and the typical symptoms of heightened immune activation were observed. Acknowledging the imperfect and incomplete relationship between antigen-stimulated DO11.10 TCR tg mice and HIV-infected humans, our data suggest that CD4⁺ T cell depletion in the setting of HIV disease may reflect, at least in part, chronic antigen exposure in the absence of proinflammatory signals and/or appropriate antigen-presenting cell functions.

INTRODUCTION

Persistent immune activation is a defining characteristic of HIV infection, both in the case of untreated and treated disease (1–3). Although the causes of such immune activation are not fully understood, they are thought to reflect changes in the mucosal barrier of the gut (4), and to underlie the loss of CD4⁺ T cells in untreated HIV-infected individuals (1–3) as well as the lack of full CD4⁺ T cell reconstitution during antiretroviral therapy (ART) (5, 6). However, given the intrinsic difficulties associated with longitudinal studies of hematolymphoid organs in humans, the impact, relative contribution, and fundamental definition of “activation” in the context of HIV disease remain unclear.

To better clarify the role of immune activation in HIV-mediated CD4⁺ T cell depletion, we turned to the DO11.10 TCR transgenic (tg) mouse model, in which >60% of peripheral CD4⁺ T cells express a transgenic TCR that recognizes OVA_{323–339} peptide (OVAp) in the context of H-2^d. We reasoned that continuous administration of OVAp to these animals might, to a certain degree, mimic the state of chronic antigen exposure found in HIV-infected humans. Accordingly, we conducted a careful analysis of T cell production and destruction across a full range of phenotypic subsets in multiple hematolymphoid organs, and quantified the fractional representation and absolute numbers of such cells as a function of time, comparing the effects of continuous antigen exposure in the presence or absence of proinflammatory stimulation provided by interleukin (IL)-1 β to recapitulate chronic activation of the innate immune system (7–9). We observed CD4⁺ T cell loss in the peripheral blood with ongoing exposure to OVAp, whether or not IL-1 β was provided concomitantly. In the absence of IL-1 β , however, we found a state of T cell depletion analogous to that observed in HIV-infected individuals, with limited expansion of effector memory T cells, depletion of CD4⁺ T cells in hematolymphoid organs, and induction of regulatory T cells (T_{REGS}). These results are discussed with respect to the known and inferred pathophysiological mechanisms implicated in untreated and treated HIV disease.

MATERIALS & METHODS

Mice

Male and female OVA TCR tg mice (DO11.10) (10), 6–12 weeks of age at the beginning of each experiment, were purchased from The Jackson Laboratory (Bar Harbor, ME, USA) and housed in the mouse facility at the University of California, San Francisco (UCSF). All data shown are from female mice aged six weeks. As these mice are not bred on a RAG^{-/-} background, they have a variable (2–32%) fraction of non-OVA-specific CD4⁺ T cells, dependent on age and location; lower fractions are present in younger mice and in peripheral lymph nodes (5–10% of CD4⁺ T cells) than in older mice and in the spleen (7–15% of CD4⁺

T cells). All experiments and procedures were approved by the UCSF Institutional Animal Care and Use Committee.

Procedures

Mice were studied longitudinally for up to seven weeks. Blood was acquired at varying time points by phlebotomy of the saphenous vein (without anesthetic). Surgery was performed under general anesthesia, using ketamine/xylazine (Wyeth, Madison, NJ, USA and Lloyd Labs Inc., Shenandoah, IA, USA). Mice were given buprenorphine (Reckitt & Colman Pharmaceuticals Inc., Richmond, VA, USA) post-operatively for pain relief. Alzet® mini-osmotic pumps (Durect Corporation, Cupertino, CA, USA) containing PBS alone, OVA_{323–339} peptide (ISQAVHAAHAEINEAGR; Biopeptide, San Diego, CA, USA) in PBS, or OVA_{323–339} peptide together with murine recombinant IL-1 β (PeproTech Inc., Rocky Hill, NJ, USA) in PBS were placed subcutaneously (s.c.) between the scapulae of DO11.10 mice. Both 14-day (model 1002) and 28-day (model 2004) pumps were used, each releasing 0.2–0.25 μ l/h of PBS or a solution containing either 0.25–1.25 μ g/ μ l OVAp in PBS (for all data shown, the concentration of OVAp was 1.25 μ g/ μ l and the total amount of peptide released per day was 6.6–7 μ g) or 0.25–1.25 μ g/ μ l OVAp in PBS together with IL-1 β (10 μ g IL-1 β / pump model 1002 and 20 μ g IL-1 β / pump model 2004 providing approximately 0.6 μ g IL-1 β / day). Pumps were equilibrated in sterile PBS according to the manufacturer's instructions for up to 48 h prior to implantation. For cross-sectional analyses of lymphoid tissue, mice were sacrificed by CO₂ asphyxiation followed by cervical dislocation. Thymus, spleen, and lymph nodes (inguinal, brachial, and axillary) were harvested and passed through mesh filters in sterile PBS with 2% FBS to obtain single cell suspensions. The absolute number of cells per organ was determined using a Coulter Counter (Beckman Coulter, Fullerton, CA, USA).

Flow cytometry

Cells from heparinized blood, lymph nodes, spleen, and thymus were stained for flow cytometric analyses using combinations of the following antibodies: (i) anti-CD4-Alexa Fluor 700 (clone L3T4), anti-CD4-allophycocyanin-Cy7 (clone L3T4), anti-CD25-PE (clone PC61), anti-CD25-allophycocyanin-Cy7 (clone PC61), anti-Ki67-FITC (clone B56), and mouse FcBlock™ (purified rat anti-mouse CD16/CD32; clone 2.4G2) (BD Pharmingen, San Jose, CA, USA); (ii) anti-CD8-Pacific Blue (clone 5H10) and anti-TCR DO11.10-allophycocyanin (clone KJ1–26) (Caltag Laboratories, Burlingame, CA, USA); and (iii) anti-FoxP3-PE (clone FJK-16s), anti-CD62L-PE-Cy7 (clone MEL-14), and anti-CD44-PE-Cy5.5 (clone IM7) (eBioscience, San Diego, CA, USA). The Live/DEAD® fixable Aqua Dead Cell Stain Kit for 405 nm excitation (Molecular Probes/Invitrogen, Eugene, Oregon, USA) was used in conjunction with Annexin V to discriminate between live, apoptotic, and dead cells. TruCount tubes (BD Biosciences, San Jose, CA, USA) were used according to the manufacturer's instructions to measure absolute peripheral blood T cell numbers. Cells were fixed after staining with either BD™ Lysing Solution (BD Biosciences, San Jose, CA, USA) for TruCount analysis or with PBS containing 2% FBS and 1% paraformaldehyde for flow cytometric analysis. For intracellular staining, cells were permeabilized with BD™ Phosflow Perm/Wash Buffer 1 (BD Biosciences, San Jose, CA, USA), which contains saponin to avoid cell fixation. Using this buffer, the incubation time for intracellular FoxP3

detection could be reduced to 1 h instead of overnight. Cells for sorting remained unfixed. Events were analyzed and/or sort-purified using an LSRII, a Digital Vantage, or a BD FACSAria™ flow cytometer (BD Biosciences, San Jose, CA, USA). Frequencies of OVA-specific (KJ1–26⁺) CD4⁺ T cell subsets were determined using FlowJo software (Tree Star Inc., Ashland, OR, USA).

In vivo T cell turnover

To measure the proliferation rate and lifespan of OVAp-stimulated T cells *in vivo*, mice with similar weight distributions across all three groups (Suppl. Fig. 1A) received a loading dose of ²H₂O (Cambridge Isotope Laboratories Inc., Andover, MA, USA) to reach 5% body water enrichment at the time of pump implantation, followed by 8% ²H₂O orally (*ad libitum*; to reach 5% body water enrichment) for a total of three days. This three-day administration protocol was designed to label C-H bonds in the deoxyribose moiety of replicating DNA in dividing cells, as described previously (11). Re-utilization of labeled ²H-deoxyribose for new DNA synthesis in purine deoxyribonucleotides is minimal (11, 12). Accordingly, this protocol results in pulse-chase incorporation of label into replicating DNA *in vivo* and allows accurate measurement of the lifespan of labeled cells. At days 3, 6, 12, and 20 after pump implantation, three mice per group were euthanized. Thymuses, lymph nodes, and spleens were harvested after blood collection from the saphenous vein. Cells were counted and stained as above, and naive (T_N: CD62L^{high}CD44^{low}) and effector memory (T_{EM}: CD62L^{low}CD44^{high}) OVA-specific CD4⁺ T cells (Suppl. Fig. 1B) were sort-purified using separated gates (Suppl. Fig. 2A) so that ²H-labeling in DNA could be measured by mass spectrometry. All analyzed cell populations were 98% pure (Suppl. Fig. 2B).

Measurement and analysis of ²H enrichment in T cell DNA

The stable isotope-based method for measuring T cell proliferation has been described in detail previously (12–14). Additional precautions and controls required for working with low cell numbers have also been developed (15). DNA from sorted cell subsets was extracted using a QIAmp DNA Micro Kit (Qiagen, Valencia, CA, USA) and hydrolyzed according to standard protocols (12–15). Deoxyribonucleosides were derivatized using pentafluorobenzyl hydroxylamine (PFBHA) solution (Sigma-Aldrich, St. Louis, MO, USA). Analysis of the derivatized deoxyribose was performed by quadrupole gas chromatography/mass spectrometry (GC/MS, Agilent 5873/6980) in negative chemical ionization mode (NCI), with helium as the carrier and methane as the reagent gas, using a DB-17 or DB-225 column (J&W Scientific, Agilent, Foster City, CA, USA). The parent ion of the pentafluoro tri-acetate (PFTA) derivative of deoxyribose has a mass-to-charge ratio (m/z) of 435 and the M1 mass isotopomer has an m/z of 436. The mole fraction of the M1 mass isotopomer was calculated as the ratio of peak areas, M1/(M0 + M1). Label incorporation in experimental samples was measured as the excess mole fraction of M1 (EM1) above the M1 mole fraction in abundance-matched unlabeled standards: $[M1/(M0 + M1)_{\text{sample}}] - [M1/(M0 + M1)_{\text{standard}}]$. The value of f, the fraction of newly synthesized DNA strands or, equivalently, the fraction of newly divided cells, was calculated as EM1/EM1*, where EM1* represents the maximal or asymptotic EM1 enrichment possible in 100% newly divided cells (13, 14). EM1* values were calculated from measured ²H enrichments in bone marrow cells (12–14).

Calculations of the fraction of labeled cells and the number of labeled cells per organ

The fraction (*f*) of labeled cells present in each organ was measured as described above. The absolute number of labeled cells per organ was calculated by multiplying the fraction of labeled cells by the total number of cells for each phenotype as determined by flow cytometry.

Statistical analysis

The two-tailed Mann-Whitney U test was used to evaluate differences between two groups. A two-way repeated measures ANOVA with the Tukey post-test to correct for multiple comparisons was used to evaluate differences across more than two groups.

RESULTS

Continuous antigenic stimulation in the presence or absence of IL-1 β results in loss of circulating T cells

The DO11.10 TCR transgenic mouse model was used to evaluate the effects of chronic antigenic stimulation on the CD4⁺ T cell compartment. These mice have a large (>60%) peripheral pool of CD4⁺ T cells that recognize OVA_{323–339} peptide in the context of H-2^d. OVA_p was administered over a period of 20 days via s.c. mini-osmotic pumps delivering ~6.8 μ g peptide/day. Absolute numbers of OVA-specific CD4⁺ T cells in the peripheral blood dropped precipitously and significantly (from ~400 cells/ μ l to <100 cells/ μ l) by day 3, and remained low for the duration of the experiment (Fig. 1A). By contrast, only a small transient dip was observed in control mice, reflecting surgical pump implantation. These patterns held across all experiments despite batch-to-batch variability in absolute cell counts (Suppl. Fig. 3). Concomitant declines were observed in the circulating OVA-specific CD4⁺ T_N and T_{EM} subsets (Figs. 1B and 1C), while the corresponding central memory (T_{CM}) cells remained numerically stable (Fig. 1D).

As this profound decline in peripheral CD4⁺ T cell numbers could reflect insufficient activation of antigen-specific cells by peptide stimulation alone, we co-administered IL-1 β with OVA_p in a separate group of mice. IL-1 β was chosen as the adjuvant for these experiments because it can be delivered continuously by s.c. mini-osmotic pumps, and because it is known to enhance the antigen-driven differentiation and expansion of CD4⁺ T cells in this mode (9). It also acts downstream of aluminum-containing adjuvants, which are routinely used and licensed for use in human vaccines (16). Again, a rapid and significant drop in circulating OVA-specific CD4⁺ T cells was observed by day 3, paralleled by a decline in the corresponding T_N cell subset (Figs. 1A and 1B). In contrast to mice receiving OVA_p alone, however, OVA-specific CD4⁺ T_{EM} cell numbers increased significantly at day 6, and then declined by day 12 to the levels observed in control mice (Fig. 1C). No changes were observed in OVA-specific T_{CM} cell numbers (Fig. 1D). Continuous s.c. administration of cognate peptide therefore depletes circulating OVA-specific CD4⁺ T cells in the presence or absence of IL-1 β , which is nevertheless required to observe an increase in the corresponding T_{EM} cell subset.

T cell depletion in the spleen and lymph nodes only occurs in the absence of IL-1 β

As circulating T cells are thought to comprise only a small fraction (<2–3%) of the total body T cell compartment, we examined the impact of chronic antigenic stimulation on CD4⁺ T cell subsets in the spleen and peripheral lymph nodes (LNs). The latter comprised pooled cells from the two brachial, axillary, and inguinal chains in each mouse. OVA_p was administered with or without IL-1 β via s.c. mini-osmotic pumps and mice were euthanized for tissue harvest at days 3, 6, 12, and 20 (n=3 mice/group/time point). Splenomegaly was evident when OVA_p was delivered in the presence but not the absence of IL-1 β (Fig. 2A), reflecting a statistically significant five-fold increase in the total number of cells per spleen (Fig. 2B). Many (35–40%) but not all of these cells were OVA-specific CD4⁺ T cells (Fig. 2C) of the T_{EM} phenotype (Fig. 2D). T_{CM} cell numbers remained low, but appeared to increase between day 12 and day 20 (Fig. 2E). At day 20, T_{CM} cell numbers were significantly higher in the spleens of mice receiving OVA_p with IL-1 β compared to those receiving OVA_p alone (Fig. 2E). Of note, the content-releasing ends of the mini-osmotic pumps were expelled after day 12 in mice that received OVA_p with IL-1 β , which may explain why CD4⁺ T cell numbers in lymphoid organs normalized to some extent in these mice by day 20. Data comparisons at the final time point are therefore strictly valid only for control mice versus those receiving OVA_p in the absence of IL-1 β .

Similar patterns were observed with pooled peripheral LNs from mice receiving OVA_p and IL-1 β , with a statistically significant increase in total cell numbers by days 6–12 (Fig. 2F), of which about 25% were OVA-specific CD4⁺ T cells (Fig. 2G). These cells were especially enriched for the T_{EM} and T_{CM} phenotypes at day 6 (Fig. 2H and 2I), whereas mice receiving OVA_p alone had higher numbers of antigen-specific T_{EM} cells at day 3 compared to those receiving IL-1 β in addition (Fig. 2H). Administration of either OVA_p alone or OVA_p with IL-1 β led to a decrease in OVA-specific T_N cells in the spleen and peripheral LNs, although a degree of recovery was noted at day 20 (Fig. 2J and 2K).

Collectively, these observations underscore the fact that depletion of OVA-specific CD4⁺ T cells in the peripheral blood is not reflective of cell numbers and/or composition in the lymphoid organs. Co-administration of OVA_p with IL-1 β caused a durable increase in OVA-specific CD4⁺ T_{EM} cells in the spleen and peripheral LNs, while administration of OVA_p alone induced only a transient increase in OVA-specific CD4⁺ T_{EM} cells in the peripheral LNs.

Loss of thymic function does not explain changes in the peripheral OVA-specific CD4⁺ T cell compartment

Given previous reports that administration of cognate peptide to TCR tg mice induces antigen-specific thymocyte depletion (10), we studied the impact of chronic OVA_p exposure on thymocyte populations over time. During the same period that administration of OVA_p alone resulted in a rapid loss of circulating CD4⁺ T cells (Fig. 1A), the total numbers of thymocytes (Fig. 3A) and of CD4⁻CD8⁻ (DN), CD4⁺CD8⁺ (DP), and CD4⁺CD8⁻ (SPCD4) thymocytes (Figs. 3B–3D) remained unchanged. By contrast, at a time (days 3–12) when mice receiving OVA_p and IL-1 β demonstrated an increase in OVA-specific CD4⁺ T cells in the spleen and peripheral LNs, there was evidence of thymocyte depletion (Figs. 3A–3D).

Although it is not clear how such depletion occurred, these observations reveal no consistent association between the cellularity of the thymus and the number and/or composition of OVA-specific CD4⁺ T cells in the periphery.

The kinetics of FoxP3⁺CD4⁺ T_{REG} induction are similar but not identical in the presence or absence of IL-1 β

As FoxP3⁺CD4⁺ T_{REGS} may influence peripheral CD4⁺ T cell homeostasis (17–19), we evaluated the fraction and absolute number of such cells as a function of time (representative flow cytometric data are shown in Suppl. Fig. 1C). In the spleen, an early (day 3–6) and significant increase in the proportion of OVA-specific (KJ1–26⁺) T_{REGS} was observed in mice receiving OVAp alone, but not in those receiving OVAp with IL-1 β (Fig. 4A). Likewise, the proportion of T_{REGS} in pooled peripheral LNs increased significantly at an early time point (day 6), more markedly and for a longer period of time (out to day 20) in mice receiving OVAp alone compared to those receiving IL-1 β in addition (Fig. 4B). When plotted as numbers per organ, these T_{REG} increases in the spleen and peripheral LNs were equivalent in the presence or absence IL-1 β (Figs. 4C and 4D). The fractional T_{REG} increase in the spleens of mice receiving OVAp alone compared to those receiving OVAp and IL-1 β was preceded by increased proliferation of T_{REGS} as measured by intracellular Ki67 staining (Fig. 4E and Suppl. Fig. 1D). The frequency of OVA-specific T_{REGS} expressing Ki67 in the peripheral LNs was also higher at early time points (days 3 and 6) in mice receiving OVAp alone compared to those receiving OVAp and IL-1 β (Fig. 4F). Moreover, a persistent fractional increase in peripheral OVA-specific CD25^{high}CD4⁺ T cells was observed in mice receiving OVAp alone, whereas the frequency of these cells increased only transiently at day 12 in mice receiving OVAp with IL-1 β (Figs. 4G). These data reveal important differences in the proportional representation and proliferation of OVA-specific T_{REGS} induced by administration of OVAp in the presence or absence of IL-1 β , and suggest that T_{REG} induction in mice treated with OVAp alone may contribute to OVA-specific CD4⁺ T cell depletion in the periphery.

Continuous antigenic stimulation induces OVA-specific CD4⁺ T cells to enter cell cycle and divide

To test the possibility that co-administration of IL-1 β might induce increased OVA-specific CD4⁺ T cell proliferation, cells were examined for expression of Ki67. Counterintuitively, Ki67 expression by OVA-specific CD4⁺ T cells in the spleen was very low (< 3%) in all groups of mice (Fig. 5A). At days 3 and 6, Ki67 expression by OVA-specific CD4⁺ T cells in the peripheral LNs was highest in mice receiving OVAp alone (Fig. 5B). High levels of Ki67 expression in the same compartment were also observed at day 3 in mice receiving OVAp with IL-1 β but these were not sustained and fell steeply to baseline levels by day 6 (Fig. 5B). In the spleen, too few Ki67⁺ OVA-specific CD4⁺ T_N, T_{EM}, and T_{CM} cells were detected to allow reliable quantification within each phenotypic subset. Sufficient cell yields were obtained from the peripheral LNs, however, and the number of Ki67⁺ OVA-specific CD4⁺ T_N cells was found to be significantly elevated at day 3 in mice receiving OVAp (Fig. 5C). At days 3 and 6, the number of Ki67⁺ OVA-specific CD4⁺ T_{EM} cells in the peripheral LNs was dramatically increased in mice receiving OVAp alone (Fig. 5D). There was a small but significant increase in the corresponding cells at days 3, 6, and 12 in mice receiving

OVAp with IL-1 β (Fig. 5D). The number of Ki67⁺ OVA-specific CD4⁺ T_{CM} cells increased at day 3 in mice receiving OVAp with or without IL-1 β (Fig. 5E). This increase was smaller than that observed for OVA-specific CD4⁺ T_N cells (Fig. 5C) and fell by day 6 close to baseline levels present in mice receiving PBS (Fig. 5E). The expression of Ki67, a putative marker of cell division, was therefore higher overall in OVA-specific CD4⁺ T cell populations from mice receiving OVAp alone.

***In vivo* proliferation of OVA-specific CD4⁺ T_N and T_{EM} cells is higher in mice receiving OVAp in the presence of IL-1 β compared to those receiving OVAp alone**

As Ki67 expression only signifies movement into the cell cycle, mice were loaded with deuterated water (²H₂O) to enable the *in vivo* measurement of new DNA synthesis (and, hence, cell division). OVA-specific CD4⁺ T_{EM} (CD62L^{low}CD44^{high}) and T_N (CD62L^{high}CD44^{low}) cells were then sort-purified from spleen or pooled peripheral LNs at multiple time points, and ²H-enriched DNA was quantified by GC-MS. Bone marrow cell ²H enrichments were determined as a reference (Suppl. Fig. 4E) and used to calculate the fraction of labeled cells. OVA-specific CD4⁺ T_{CM} cells were not sorted, as they constituted a very small population (Fig. 1D, 2E and 2I). Although OVAp alone increased the proliferation of OVA-specific CD4⁺ T_{EM} cells compared to mice receiving PBS, a significantly higher proportion of these cells in the spleen and peripheral LNs incorporated ²H by day 6 in mice receiving OVAp with IL-1 β (Fig. 6A and 6B). In each organ, this cell division led to a statistically significant increase in the total number of newly divided T_{EM} cells (Figs. 6C and 6D). As this is one of the cell populations that increased most markedly over time (Figs. 2D and 2H), it seems likely that this difference can be attributed to the induction of proliferation by IL-1 β .

Reciprocally, the administration of OVAp in the absence of IL-1 β may trigger movement into the cell cycle, as evidenced by increased Ki67 expression in peripheral LN-resident T_{EM} cells (Figure 5D), but only limited proliferation. In support of this model, the percentage and number of new T_{EM} cells remaining did not decrease between days 6 and 12 in the peripheral LNs of mice receiving OVAp alone (Fig. 6F and 6H), and the decrease in labeled T_{EM} cells in the spleen appeared to be less than that observed in control mice receiving PBS (Fig. 6E and 6G). These data are consistent with a lack of input from unlabeled, newly divided cells between days 6 and 12. Concomitantly, labeled T_{EM} cells in the spleen and peripheral LNs declined to a significantly greater extent in mice receiving OVAp with IL-1 β (Fig. 6E and 6F), indicating continued input of newly divided, unlabeled cells with IL-1 β treatment. Moreover, at days 12–20, a loss of total labeled T_{EM} cells in the spleen and peripheral LNs was observed both in mice receiving OVAp alone and in mice receiving OVAp with IL-1 β (Fig. 6G and 6H), indicating death of newly divided cells consistent with the dissipation of IL-1 β effects and normalization of cell counts subsequent to pump expulsion in the latter group by day 12. ²H enrichments in T_N cells from the peripheral LNs were similar and increased at day 3 together with the fraction of labeled T_N cells in both the OVAp alone and OVAp with IL-1 β groups (Suppl. Fig. 4A and 4C). By contrast, the fraction of labeled T_N cells in the spleen did not increase significantly despite apparent ²H enrichments at day 3 both in mice receiving OVAp alone and in mice receiving OVAp with IL-1 β (Suppl. Fig. 4B and 4D).

As expected, the overall fractions of labeled T_N cells were lower than the corresponding fractions of labeled T_{EM} cells (Fig. 6A and 6B, Suppl. Fig. 4C and 4D). The increase in the fraction of labeled T_N cells in the peripheral LNs was still apparent at day 6 in mice receiving OVAp with IL-1 β (Suppl. Fig. 4C). As the number of T_N cells decreased, it is most likely that they converted to T_{EM} cells with further division. 2H incorporation in T_N cells from mice receiving PBS alone increased over time (Suppl. Fig. 4A and 4C). Similar findings have been reported for T_N cells derived from human peripheral blood (20), almost certainly reflecting slow division rates that lead to the progressive accumulation of labeled cells in this compartment.

Collectively, these kinetic results reinforce the cell count findings and show that *de novo* cell division in this model depends on the presence of both OVAp and IL-1 β .

DISCUSSION

One of the unanswered questions regarding the pathogenesis of HIV infection is whether chronic antigenic stimulation *per se* leads to $CD4^+$ T cell depletion. Here, we provide data gathered from a mouse model suggesting that antigen-specific $CD4^+$ T cells are indeed lost during a period of continuous antigenic exposure, but that such loss may only occur within hemolymphoid organs when antigen is provided without engagement of important direct and indirect contributions from the innate immune system (e.g., those induced by concomitant administration of the prototypic proinflammatory cytokine IL-1 β). We chose DO11.10 TCR tg mice for these experiments because they harbor high frequencies of $CD4^+$ T cells that recognize OVA in the context of H-2^d. This trait allowed a systematic study of circulating and tissue-resident $CD4^+$ T cells responding to a defined antigenic stimulus over time. Using implanted s.c. mini-osmotic pumps, these mice were exposed continuously to OVA_{323–339} peptide (OVAp) for 20 days, with or without IL-1 β . In both instances, OVA-specific $CD4^+$ T cell counts dropped in the peripheral blood. In the presence of IL-1 β , however, such depletion of the circulating $CD4^+$ T cell pool was accompanied by a marked and significant increase in the absolute number of OVA-specific $CD4^+$ T cells found in the spleen, which in turn was associated with a higher absolute number of dividing T_{EM} cells (as evidenced by increased incorporation of deuterated water into newly synthesized DNA). By contrast, mice receiving OVAp in the absence of IL-1 β showed no such increase in the absolute number of OVA-specific $CD4^+$ T cells in the spleen (although they did show a transient increase in LN cellularity due to an increase in OVA-specific $CD4^+$ T cells, mostly of the T_{EM} phenotype). Cell division was initiated in mice receiving OVAp alone, as evidenced by increased Ki67 expression and deuterium incorporation, but this did not lead to an increase in OVA-specific $CD4^+$ T_{EM} cell numbers in the spleen. These changes in T cell homeostasis were accompanied by evidence of greater FoxP3⁺ T_{REG} induction in mice receiving OVAp in the absence of IL-1 β . In sum, the presence of IL-1 β was associated with cell division and an increase in the absolute number of OVA-specific $CD4^+$ T_{EM} cells, even though $CD4^+$ T cell depletion was observed in the peripheral blood. By contrast, continuous exposure to antigen in the absence of innate immune activation resulted in conditions most analogous to those found in the setting of HIV disease. Notably, none of these changes were easily relatable to the size and function of the thymus in these young adult mice.

Substantial differences clearly exist between antigen-stimulated DO11.10 TCR tg mice and HIV-infected humans. In particular, most of the CD4⁺ T cells lost in the context of HIV infection are not specific for the virus, which itself is a major cause of the observed immunopathology (21). Moreover, a range of mechanisms beyond direct viral cytopathogenicity likely contribute to the process of CD4⁺ T cell depletion in HIV-infected individuals, including the diverse effects of other proinflammatory cytokines (e.g., IFN α , TNF) (22, 23), type I interferons (24), and microbial translocation (25, 26), as well as alternative forms of cell death (e.g., pyroptosis) (27). These multifactorial causes of CD4⁺ T cell lymphopenia are not recapitulated in DO11.10 TCR tg mice. Nonetheless, this simplified model allowed an unfettered evaluation of CD4⁺ T cell dynamics in the presence of continuous antigenic stimulation. Acknowledging the many caveats, how might our findings relate to the disposition and fate of CD4⁺ T cells in the setting of HIV disease?

It has long been noted that the number of circulating CD4⁺ T cells declines inexorably as a function of disease progression in most HIV-infected individuals, providing a remarkably accurate barometer for the ultimate susceptibility of the patient to opportunistic infections and, historically, a definition of “AIDS” when the circulating CD4⁺ T cell count falls below 200 cells/ μ l (28, 29). However, it remains unclear whether and to what extent the circulating CD4⁺ T cell count reflects the number of CD4⁺ T cells found within fixed hematolymphoid compartments. Indeed, lymphadenopathy is a pathognomonic clinical sign of progressive disease (30) and early radiographic studies noted evidence of abdominal lymphadenopathy in HIV-infected patients as well (31), suggesting that CD4⁺ T cells are sequestered to lymphoid tissues. Alternatively, or in addition, CD4⁺ T cells may be lost from the circulation due to: (i) loss of progenitor activity in the bone marrow and/or thymus; (ii) loss of homeostatic mechanisms that normally sustain T cell proliferation in the periphery; (iii) sequestration/redistribution of CD4⁺ T cells into extravascular spaces that are not usually assessed in HIV-infected individuals; (iv) killing of HIV-infected CD4⁺ T cells by HIV-specific cytotoxic CD8⁺ T cells; and (v) killing of “bystander” CD4⁺ T cells by unknown mechanisms (32). Finally, although there have been numerous studies over the past 20 years to document the proliferation and activation status of T cells in the setting of HIV disease (33), there are scant quantitative or qualitative data showing that “activated” cells are actually moving through multiple rounds of proliferation. Thus, the fraction of cells positive for Ki67 (or other markers of cell division) has been found to be high at times when the circulating CD4⁺ T cell count is low, leading to the inference that CD4⁺ T cell division is high (34, 35). On the other, the absolute number of CD4⁺ T cells positive for Ki67 or incorporating deuterated glucose is inappropriately low in late-stage disease (13), suggesting a block on cell division instead.

Our observations in the OVA TCR tg model raise several interesting possibilities that might be pertinent to the pathophysiology of HIV disease. First, it is clear that continuous antigenic exposure results in depletion of circulating CD4⁺ T cells in this model, whether or not IL-1 β is present. Yet, it is only in the absence of IL-1 β that total body CD4⁺ T cell loss is observed. Such loss is associated with evidence that cells can begin to move through the cell cycle (i.e., express Ki67) but that they then do not divide (i.e., incorporate ²H into new strands of DNA), as has been observed in the circulating cells of HIV-infected subjects by Sieg and colleagues (36). At the same time, there is a relative increase in CD4⁺ T_{REGS}, as

has also been observed in those infected with HIV (37). In the presence of IL-1 β , by contrast, T cell division is enhanced in the spleen and peripheral LNs, consistent with a qualitatively distinct mechanism of T cell homeostasis.

As the difference between the two states is related to the presence or absence of IL-1 β , it is tempting to speculate that continuous antigen exposure in the absence of IL-1 β (or, more generally, co-stimulation) leads to total body CD4⁺ T cell depletion. In this scenario, both the cytopathic effects of HIV on CD4⁺ T cells and the deleterious impact of HIV infection on CD4⁺ myeloid cells (including antigen-presenting cells) capable of IL-1 β production (38) might cumulatively lead to altered homeostasis of the T cell lineage, with less cell division over time. Although further work is clearly required to extend these findings to humans (e.g., in studies examining IL-1 β blockade in the context of treated HIV disease) (39), our data suggest that interventions designed to restore innate immunity in general (or the production of IL-1 β in particular) might help to reinstate complete T cell immunity in patients treated with ART.

Supplementary Material

Refer to Web version on PubMed Central for supplementary material.

ACKNOWLEDGEMENTS

We would like to thank George Chkhenkeli and José Rivera for technical help, Cheryl Stoddart, Sofiya Galkina, and Mary Beth Moreno for advice and resource provision, and Marty Bigos, Tomasz Poplonski, Valerie Stepps and Ck Poon for flow cytometry services.

Abbreviations used in this paper

T_N	naive T cells
T_{CM}	central memory T cells
T_{EM}	effector memory T cells
T_{REG}	regulatory T cells
tg	transgenic
AICD	activation-induced cell death
THY	thymus
SPL	spleen
LNs	lymph nodes

REFERENCES

1. Deeks SG, Kitchen CM, Liu L, Guo H, Gascon R, Narvaez AB, Hunt P, Martin JN, Kahn JO, Levy J, McGrath MS, Hecht FM. Immune activation set point during early HIV infection predicts subsequent CD4⁺ T-cell changes independent of viral load. *Blood*. 2004; 104:942–947. [PubMed: 15117761]

2. Fahey JL, Taylor JM, Detels R, Hofmann B, Melmed R, Nishanian P, Giorgi JV. The prognostic value of cellular and serologic markers in infection with human immunodeficiency virus type 1. *N Engl J Med.* 1990; 322:166–172. [PubMed: 1967191]
3. Hazenberg MD, Otto SA, van Benthem BH, Roos MT, Coutinho RA, Lange JM, Hamann D, Prins M, Miedema F. Persistent immune activation in HIV-1 infection is associated with progression to AIDS. *AIDS.* 2003; 17:1881–1888. [PubMed: 12960820]
4. Brenchley JM, Price DA, Schacker TW, Asher TE, Silvestri G, Rao S, Kazzaz Z, Bornstein E, Lambotte O, Altmann D, Blazar BR, Rodriguez B, Teixeira-Johnson L, Landay A, Martin JN, Hecht FM, Picker LJ, Lederman MM, Deeks SG, Douek DC. Microbial translocation is a cause of systemic immune activation in chronic HIV infection. *Nat Med.* 2006; 12:1365–1371. [PubMed: 17115046]
5. Hunt PW, Martin JN, Sinclair E, Bredt B, Hagos E, Lampiris H, Deeks SG. T cell activation is associated with lower CD4+ T cell gains in human immunodeficiency virus-infected patients with sustained viral suppression during antiretroviral therapy. *J Infect Dis.* 2003; 187:1534–1543. [PubMed: 12721933]
6. Kelley CF, Kitchen CM, Hunt PW, Rodriguez B, Hecht FM, Kitahata M, Crane HM, Willig J, Mugavero M, Saag M, Martin JN, Deeks SG. Incomplete peripheral CD4+ cell count restoration in HIV-infected patients receiving long-term antiretroviral treatment. *Clin Infect Dis.* 2009; 48:787–794. [PubMed: 19193107]
7. Philbin VJ, Levy O. Developmental biology of the innate immune response: implications for neonatal and infant vaccine development. *Pediatr Res.* 2009; 65:98R–105R.
8. Martinon F, Mayor A, Tschopp J. The inflammasomes: guardians of the body. *Annu Rev Immunol.* 2009; 27:229–265. [PubMed: 19302040]
9. Ben-Sasson SZ, Hu-Li J, Quiel J, Cauchetaux S, Ratner M, Shapira I, Dinarello CA, Paul WE. IL-1 acts directly on CD4 T cells to enhance their antigen-driven expansion and differentiation. *Proc Natl Acad Sci U S A.* 2009; 106:7119–7124. [PubMed: 19359475]
10. Murphy KM, Heimberger AB, Loh DY. Induction by antigen of intrathymic apoptosis of CD4+CD8+TCR α thymocytes in vivo. *Science.* 1990; 250:1720–1723. [PubMed: 2125367]
11. Macallan DC, Fullerton CA, Neese RA, Haddock K, Park SS, Hellerstein MK. Measurement of cell proliferation by labeling of DNA with stable isotope-labeled glucose: studies in vitro, in animals, and in humans. *Proc Natl Acad Sci U S A.* 1998; 95:708–713. [PubMed: 9435257]
12. McCune JM, Hanley MB, Cesar D, Halvorsen R, Hoh R, Schmidt D, Wieder E, Deeks S, Siler S, Neese R, Hellerstein M. Factors influencing T-cell turnover in HIV-1-seropositive patients. *J Clin Invest.* 2000; 105:R1–R8. [PubMed: 10712441]
13. Hellerstein M, Hanley MB, Cesar D, Siler S, Papageorgopoulos C, Wieder E, Schmidt D, Hoh R, Neese R, Macallan D, Deeks S, McCune JM. Directly measured kinetics of circulating T lymphocytes in normal and HIV-1-infected humans. *Nat Med.* 1999; 5:83–89. [PubMed: 9883844]
14. Neese RA, Siler SQ, Cesar D, Antelo F, Lee D, Misell L, Patel K, Tehrani S, Shah P, Hellerstein MK. Advances in the stable isotope-mass spectrometric measurement of DNA synthesis and cell proliferation. *Anal Biochem.* 2001; 298:189–195. [PubMed: 11700973]
15. Busch R, Neese RA, Awada M, Hayes GM, Hellerstein MK. Measurement of cell proliferation by heavy water labeling. *Nat Protoc.* 2007; 2:3045–3057. [PubMed: 18079703]
16. Sokolovska A, Hem SL, HogenEsch H. Activation of dendritic cells and induction of CD4(+) T cell differentiation by aluminum-containing adjuvants. *Vaccine.* 2007; 25:4575–4585. [PubMed: 17485153]
17. Almeida AR, Legrand N, Papiernik M, Freitas AA. Homeostasis of peripheral CD4+ T cells: IL-2R α and IL-2 shape a population of regulatory cells that controls CD4+ T cell numbers. *J Immunol.* 2002; 169:4850–4860. [PubMed: 12391195]
18. Annacker O, Pimenta-Araujo R, Burlen-Defranoux O, Barbosa TC, Cumano A, Bandeira A. CD25+ CD4+ T cells regulate the expansion of peripheral CD4 T cells through the production of IL-10. *J Immunol.* 2001; 166:3008–3018. [PubMed: 11207250]
19. Dahlberg PE, Schartner JM, Timmel A, Seroogy CM. Daily subcutaneous injections of peptide induce CD4+ CD25+ T regulatory cells. *Clin Exp Immunol.* 2007; 149:226–234. [PubMed: 17490400]

20. Hellerstein MK, Hoh RA, Hanley MB, Cesar D, Lee D, Neese RA, McCune JM. Subpopulations of long-lived and short-lived T cells in advanced HIV-1 infection. *J Clin Invest*. 2003; 112:956–966. [PubMed: 12975480]
21. Douek DC, Roederer M, Koup RA. Emerging concepts in the immunopathogenesis of AIDS. *Annu Rev Med*. 2009; 60:471–484. [PubMed: 18947296]
22. Herbeuval JP, Shearer GM. HIV-1 immunopathogenesis: how good interferon turns bad. *Clin Immunol*. 2007; 123:121–128. [PubMed: 17112786]
23. Keating SM, Jacobs ES, Norris PJ. Soluble mediators of inflammation in HIV and their implications for therapeutics and vaccine development. *Cytokine Growth Factor Rev*. 2012; 23:193–206. [PubMed: 22743035]
24. Sandler NG, Bosinger SE, Estes JD, Zhu RT, Tharp GK, Boritz E, Levin D, Wijeyesinghe S, Makamdop KN, del Prete GQ, Hill BJ, Timmer JK, Reiss E, Yarden G, Darko S, Contijoch E, Todd JP, Silvestri G, Nason M, Norgren RB Jr, Keele BF, Rao S, Langer JA, Lifson JD, Schreiber G, Douek DC. Type I interferon responses in rhesus macaques prevent SIV infection and slow disease progression. *Nature*. 2014; 511:601–605. [PubMed: 25043006]
25. Brechley JM, Price DA, Douek DC. HIV disease: fallout from a mucosal catastrophe? *Nat Immunol*. 2006; 7:235–239. [PubMed: 16482171]
26. Marchetti G, Tincati C, Silvestri G. Microbial translocation in the pathogenesis of HIV infection and AIDS. *Clin Microbiol Rev*. 2013; 26:2–18. [PubMed: 23297256]
27. Doitsh G, Galloway NL, Geng X, Yang Z, Monroe KM, Zepeda O, Hunt PW, Hatano H, Sowinski S, Munoz-Arias I, Greene WC. Cell death by pyroptosis drives CD4 T-cell depletion in HIV-1 infection. *Nature*. 2014; 505:509–514. [PubMed: 24356306]
28. MacDonell KB, Chmiel JS, Poggensee L, Wu S, Phair JP. Predicting progression to AIDS: combined usefulness of CD4 lymphocyte counts and p24 antigenemia. *Am J Med*. 1990; 89:706–712. [PubMed: 1979205]
29. Chang SW, Kate MH, Hernandez SR. The new AIDS case definition. Implications for San Francisco. *JAMA*. 1992; 267:973–975. [PubMed: 1346406]
30. Redfield RR, Wright DC, Tramont EC. The Walter Reed staging classification for HTLV-III/LAV infection. *N Engl J Med*. 1986; 314:131–132. [PubMed: 2934633]
31. Knollmann FD, Maurer J, Grunewald T, Schedel H, Vogl TJ, Pohle HD, Felix R. Abdominal CT features and survival in acquired immunodeficiency. *Acta Radiol*. 1997; 38:970–977. [PubMed: 9394651]
32. McCune JM. The dynamics of CD4+ T-cell depletion in HIV disease. *Nature*. 2001; 410:974–979. [PubMed: 11309627]
33. Klatt NR, Chomont N, Douek DC, Deeks SG. Immune activation and HIV persistence: implications for curative approaches to HIV infection. *Immunol Rev*. 2013; 254:326–342. [PubMed: 23772629]
34. Anthony KB, Yoder C, Metcalf JA, DerSimonian R, Orenstein JM, Stevens RA, Falloon J, Polis MA, Lane HC, Sereti I. Incomplete CD4 T cell recovery in HIV-1 infection after 12 months of highly active antiretroviral therapy is associated with ongoing increased CD4 T cell activation and turnover. *J Acquir Immune Defic Syndr*. 2003; 33:125–133. [PubMed: 12794543]
35. Ribeiro RM, Mohri H, Ho DD, Perelson AS. In vivo dynamics of T cell activation, proliferation, and death in HIV-1 infection: why are CD4+ but not CD8+ T cells depleted? *Proc Natl Acad Sci U S A*. 2002; 99:15572–15577. [PubMed: 12434018]
36. Sieg SF, Bazdar DA, Lederman MM. S-phase entry leads to cell death in circulating T cells from HIV-infected persons. *J Leukoc Biol*. 2008; 83:1382–1387. [PubMed: 18372341]
37. Simonetta F, Bourgeois C. CD4+FOXP3+ Regulatory T-Cell Subsets in Human Immunodeficiency Virus Infection. *Front Immunol*. 2013; 4:215. [PubMed: 23908654]
38. Ortiz AM, DiNapoli SR, Brechley JM. Macrophages Are Phenotypically and Functionally Diverse across Tissues in Simian Immunodeficiency Virus-Infected and Uninfected Asian Macaques. *J Virol*. 2015; 89:5883–5894. [PubMed: 25787286]
39. Botsios C. Safety of tumour necrosis factor and interleukin-1 blocking agents in rheumatic diseases. *Autoimmun Rev*. 2005; 4:162–170. [PubMed: 15823502]

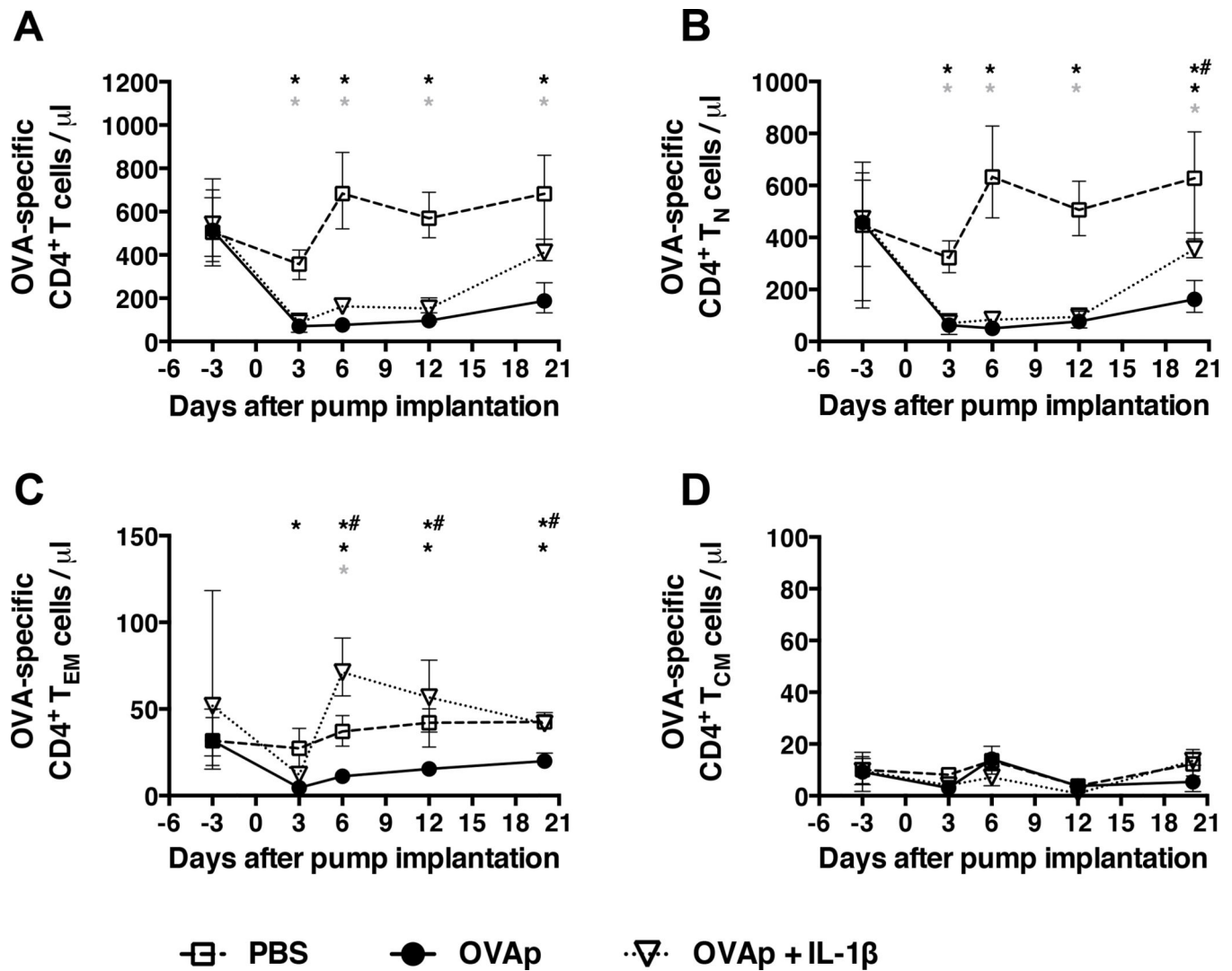


Figure 1. Continuous antigenic stimulation in the presence or absence of IL-1 β results in loss of circulating CD4⁺ T cells

Mini-osmotic pumps containing either PBS, OVAp in PBS, or OVAp together with IL-1 β in PBS were implanted s.c. between the scapulae of DO11.10 TCR tg mice and, at the indicated time points, the numbers of (A) OVA-specific (KJ1-26⁺) CD4⁺ T cells, (B) OVA-specific CD4⁺ T_N cells, (C) OVA-specific CD4⁺ T_{EM} cells, and (D) OVA-specific CD4⁺ T_{CM} cells were assessed per μ l of peripheral blood using Trucount tubes (BD Biosciences). Data shown are from three mice per group per time point, and are representative of three similar experiments for the PBS and OVAp groups (Suppl. Fig. 3). Shown are means and ranges. *, p<0.05 PBS versus OVAp; grey asterisk, p<0.05 PBS versus OVAp + IL-1 β ; #, p<0.05 OVAp versus OVAp + IL-1 β . Statistical analysis was conducted using a two-way ANOVA with the Tukey post-test to correct for multiple comparisons.

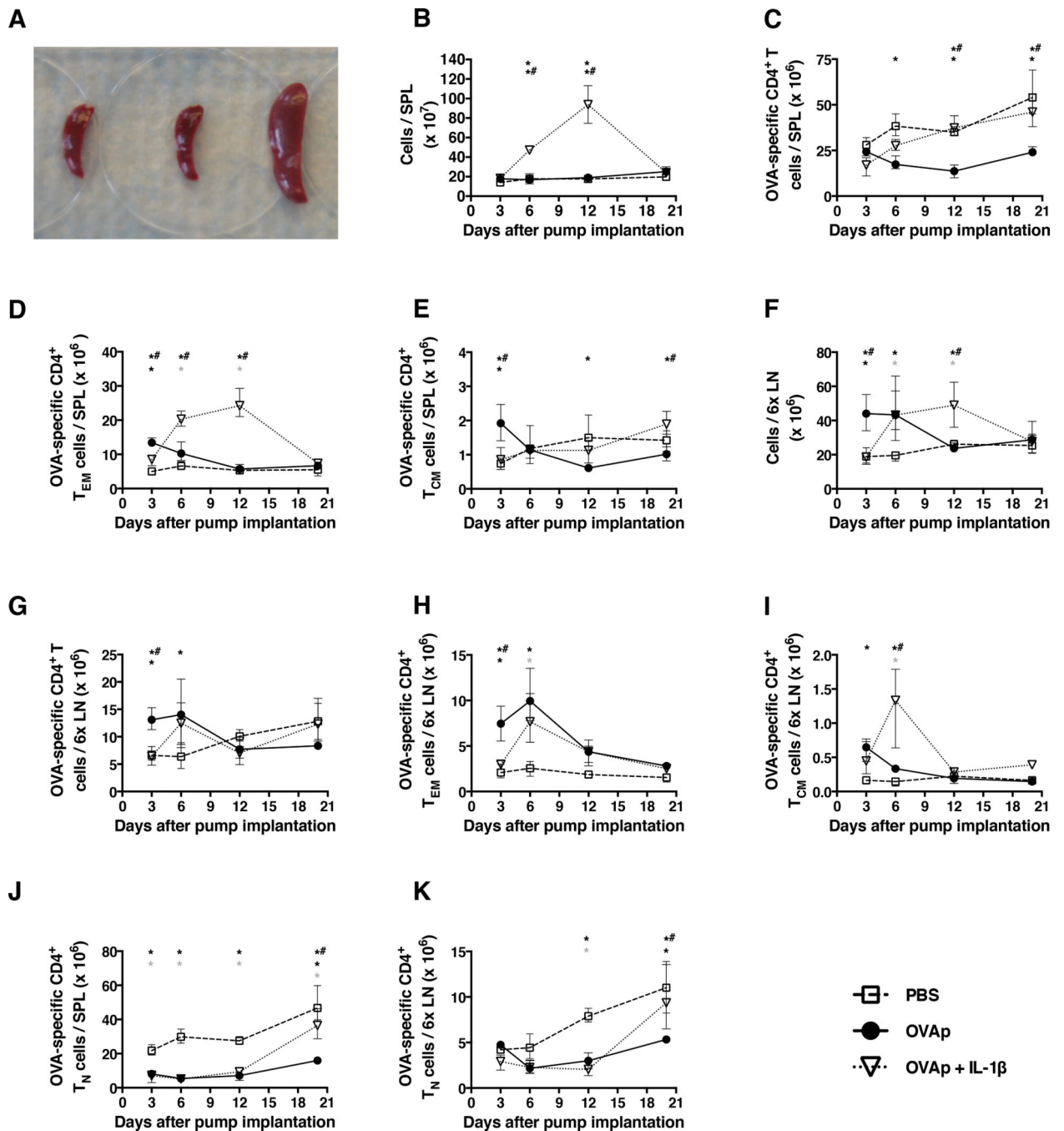


Figure 2. CD4⁺ T cell depletion in the spleen and lymph nodes only occurs in the absence of IL-1 β

Mice were implanted with mini-osmotic pumps as per the legend for Fig. 1. (A) Representative spleens from PBS (far left), OVAp (middle), and OVAp with IL-1 β mice collected at day 12. Splenomegaly was already observed at day 6 in mice receiving OVAp with IL-1 β . The spleens are shown on a 6-well tissue culture plate. Numbers of (B) spleen cells, (C) OVA-specific CD4⁺ T cells per spleen, (D) OVA-specific CD4⁺ T_{EM} cells per spleen, (E) OVA-specific CD4⁺ T_{CM} cells per spleen, (F) pooled peripheral LNs (2x

brachial, 2x axillary, 2x inguinal) cells, **(G)** OVA-specific CD4⁺ T cells per peripheral LN pool, **(H)** OVA-specific CD4⁺ T_{EM} cells per peripheral LN pool, **(I)** OVA-specific CD4⁺ T_{CM} cells per peripheral LN pool, **(J)** OVA-specific CD4⁺ T_N cells per spleen, and **(K)** OVA-specific CD4⁺ T_N cells per peripheral LN pool. Data shown are from the same experiment shown in Fig. 1. Shown are means and ranges. *, p<0.05 PBS versus OVAp; grey asterix, p<0.05 PBS versus OVAp + IL-1 β ; *#, p<0.05 OVAp versus OVAp + IL-1 β . Statistical analysis was conducted using a two-way ANOVA with the Tukey post-test to correct for multiple comparisons.

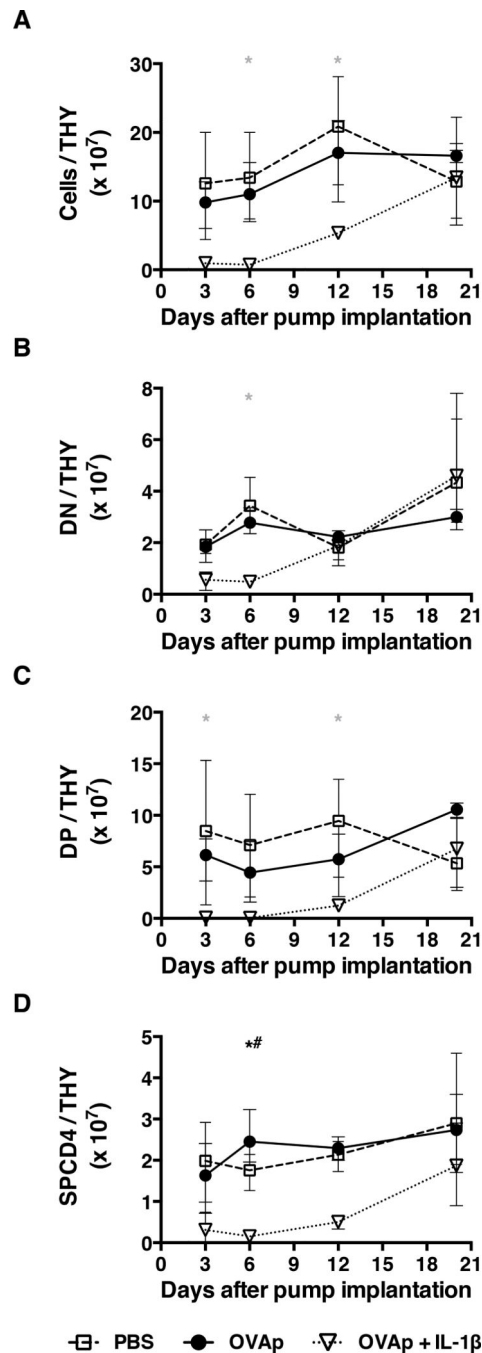


Figure 3. Loss of thymic function does not explain changes in the peripheral OVA-specific CD4⁺ T cell compartment

Mice were implanted with mini-osmotic pumps as per the legend for Fig. 1. At four time points thereafter, thymuses (THY) were removed from individual mice to count the numbers of (A) total cells, (B) DN thymocytes, (C) DP thymocytes, and (D) SPCD4 thymocytes. Data shown are from the same experiment shown in Fig. 1. Shown are means and ranges. *, $p < 0.05$ PBS versus OVAp; grey asterisk, $p < 0.05$ PBS versus OVAp + IL-1 β ; $\#\#$, $p < 0.05$ OVAp versus OVAp + IL-1 β . Statistical analysis was conducted using a two-way ANOVA with the Tukey post-test to correct for multiple comparisons.

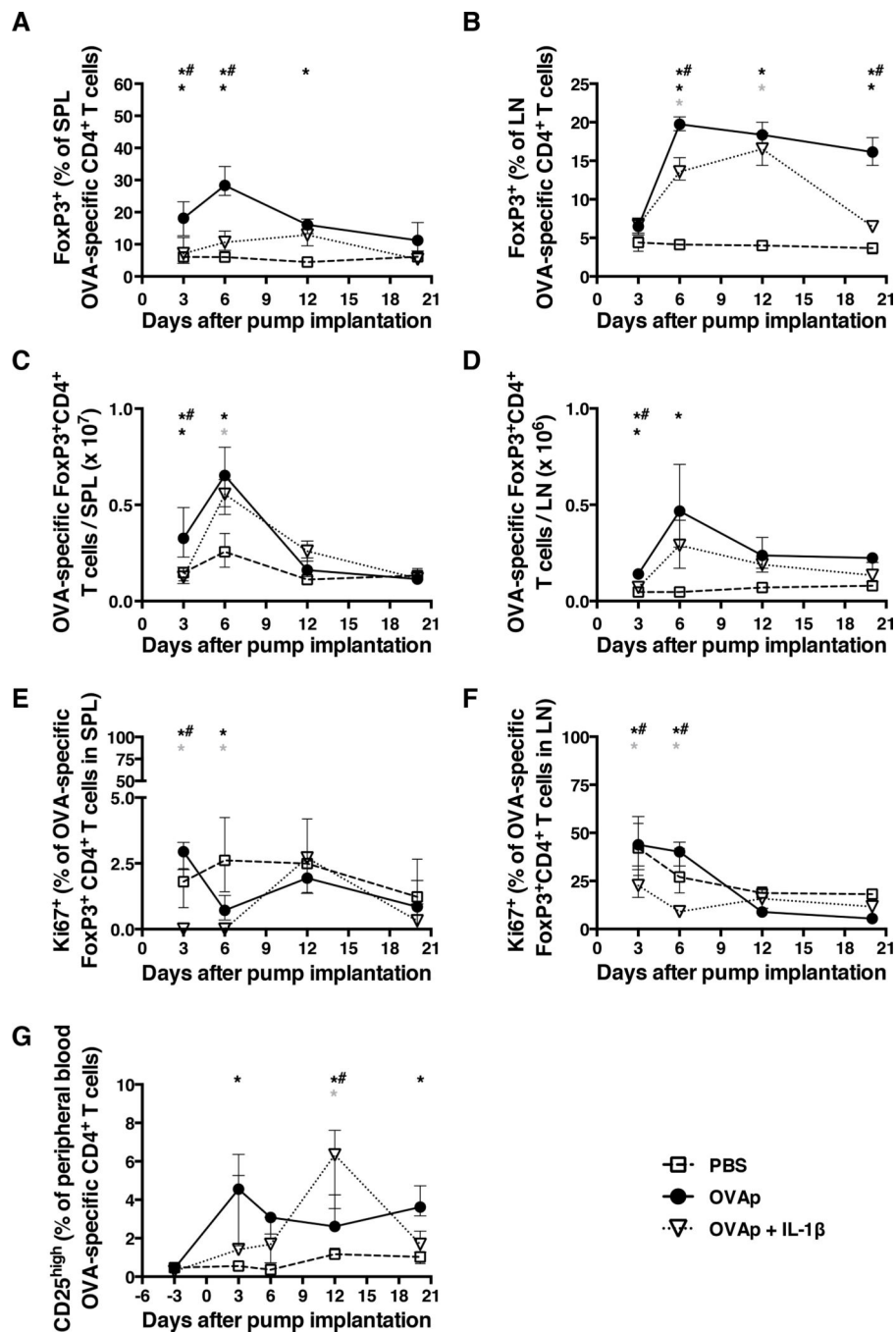


Figure 4. The kinetics of FoxP3⁺CD4⁺ T_{REG} induction are similar but non-identical in the presence or absence of IL-1β

Mice were implanted with mini-osmotic pumps as per the legend for Fig. 1. At four time points thereafter, peripheral blood and the indicated tissues were collected to determine (A) the frequency of OVA-specific FoxP3⁺CD4⁺ T cells in the spleen, (B) the frequency of OVA-specific FoxP3⁺CD4⁺ T cells in peripheral LNs, (C) the number of OVA-specific FoxP3⁺CD4⁺ T cells in the spleen, (D) the number of OVA-specific FoxP3⁺CD4⁺ T cells in peripheral LNs, (E) the frequency of OVA-specific FoxP3⁺CD4⁺ T cells expressing Ki67 in

the spleen, **(F)** the frequency of OVA-specific FoxP3⁺CD4⁺ T cells expressing Ki67 in peripheral LNs, and **(G)** the frequency of OVA-specific CD25^{high}CD4⁺ T cells in the peripheral blood. Data shown are from the same experiment shown in Fig. 1. Shown are means and ranges. *, p<0.05 PBS versus OVAp; grey asterix, p<0.05 PBS versus OVAp + IL-1 β ; *#, p<0.05 OVAp versus OVAp + IL-1 β . Statistical analysis was conducted using a two-way ANOVA with the Tukey post-test to correct for multiple comparisons.

Author Manuscript

Author Manuscript

Author Manuscript

Author Manuscript

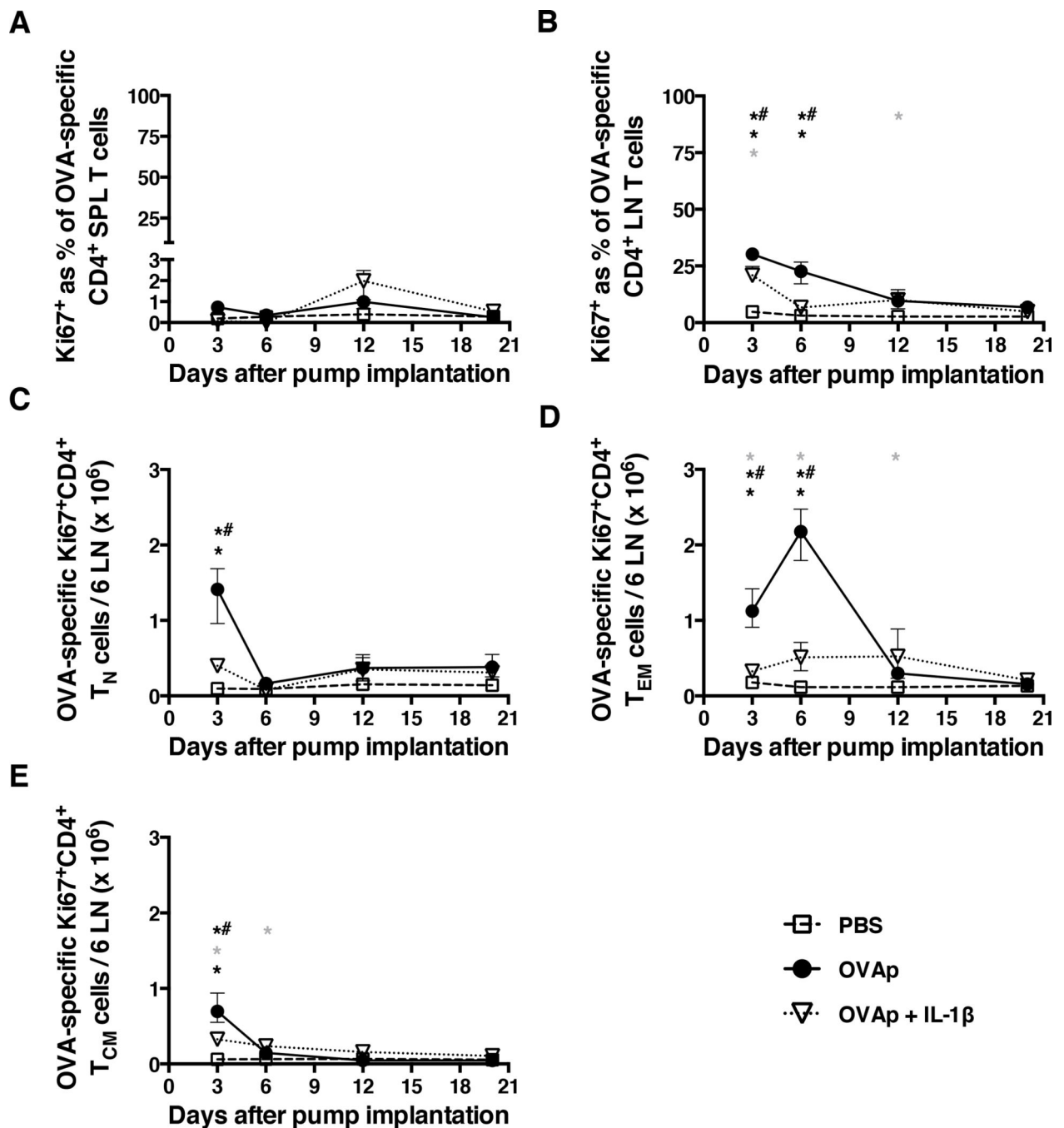


Figure 5. Continuous antigenic stimulation induces OVA-specific CD4⁺ T cells to enter cell cycle Mice were implanted with mini-osmotic pumps as per the legend for Fig. 1. At the indicated time points, spleens and peripheral LNs were collected to determine (A) the percentage of Ki67⁺ OVA-specific CD4⁺ T cells in the spleen, (B) the percentage of Ki67⁺ OVA-specific CD4⁺ T cells in peripheral LNs, (C) the number of Ki67⁺ OVA-specific CD4⁺ T_N cells in peripheral LNs, (D) the number of Ki67⁺ OVA-specific CD4⁺ T_{EM} cells in peripheral LNs, and (E) the number of Ki67⁺ OVA-specific CD4⁺ T_{CM} cells in peripheral LNs. Data shown are from the same experiment shown in Figure 1. Shown are means and ranges. *, p<0.05

PBS versus OVAp; grey asterix, $p < 0.05$ PBS versus OVAp + IL-1 β ; *#, $p < 0.05$ OVAp versus OVAp + IL-1 β . Statistical analysis was conducted using a two-way ANOVA with the Tukey post-test to correct for multiple comparisons.

Author Manuscript

Author Manuscript

Author Manuscript

Author Manuscript

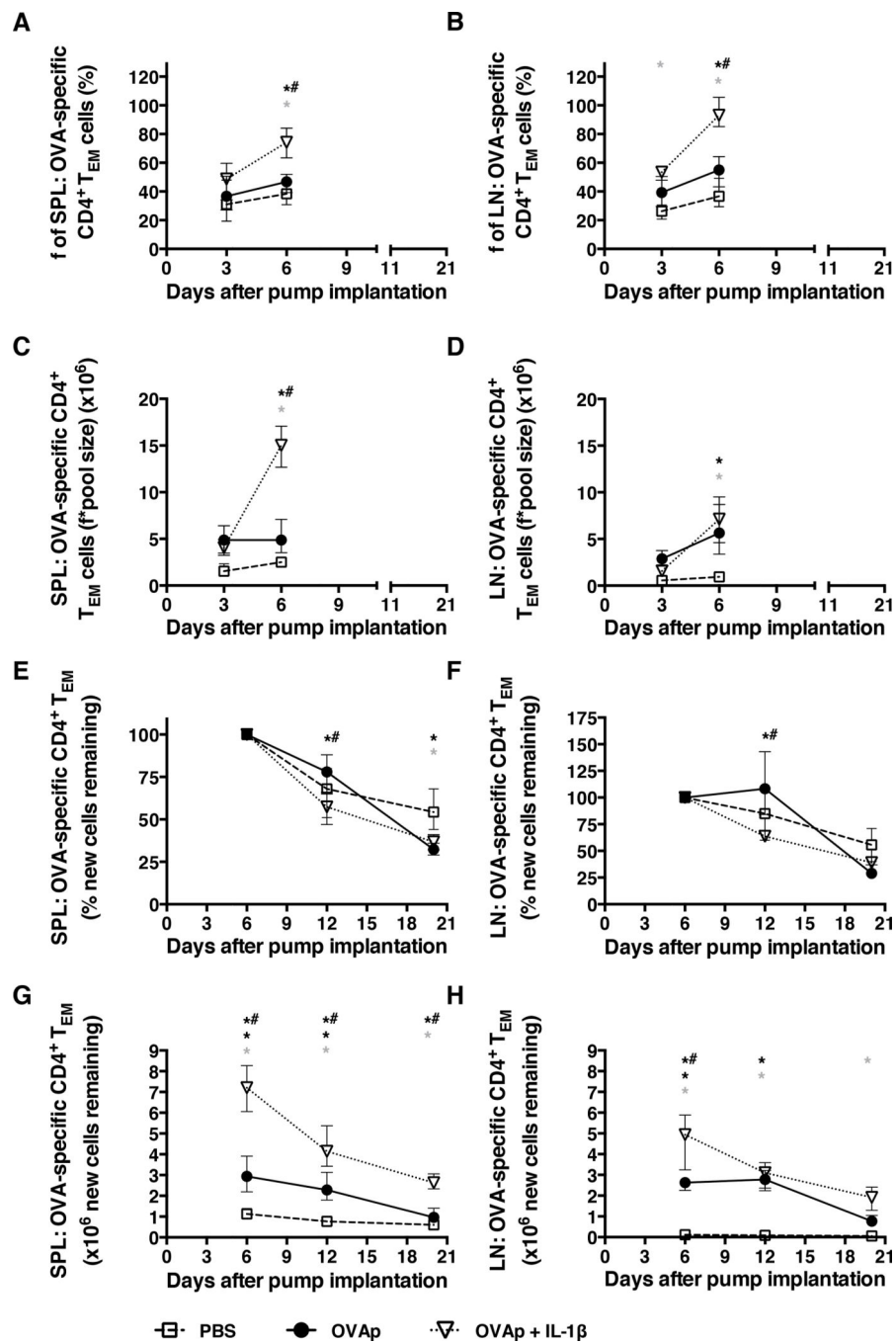


Figure 6. *In vivo* proliferation of OVA-specific T_{EM} cells is higher in mice receiving OVAp and IL-1 β compared to those receiving OVAp alone

After an intraperitoneal loading dose of 2H_2O to reach 5% body water enrichment, mice were labeled orally with 2H_2O provided in drinking water for the first 72 h after mini-osmotic pump implantation as per the legend for Fig. 1. (A) The fraction of labeled OVA-specific $CD4^+$ T_{EM} cells in the spleen. (B) The fraction of labeled OVA-specific $CD4^+$ T_{EM} cells in peripheral LNs. (C) The number of labeled OVA-specific $CD4^+$ T_{EM} cells in the spleen. (D) The number of labeled OVA-specific $CD4^+$ T_{EM} cells in peripheral LNs. (E)

The percentage of new OVA-specific CD4⁺ T_{EM} cells remaining in the spleen. **(F)** The percentage of new OVA-specific CD4⁺ T_{EM} cells remaining in peripheral LNs. **(G)** The number of new OVA-specific CD4⁺ T_{EM} cells remaining in the spleen. **(H)** The number of new OVA-specific CD4⁺ T_{EM} cells remaining in peripheral LNs. Data shown are from the same experiment shown in Fig. 1. Shown are means and ranges. *, p<0.05 PBS versus OVAp; grey asterix, p<0.05 PBS versus OVAp + IL-1β; *#, p<0.05 OVAp versus OVAp + IL-1β. Statistical analysis was conducted using a two-way ANOVA with the Tukey post-test to correct for multiple comparisons.